

University of Groningen

Causes of variation of darkness in flocks of starlings, a computational model

Costanzo, A.; Hildenbrandt, H.; Hemelrijk, C. K.

Published in:
Swarm intelligence

DOI:
[10.1007/s11721-021-00207-4](https://doi.org/10.1007/s11721-021-00207-4)

IMPORTANT NOTE: You are advised to consult the publisher's version (publisher's PDF) if you wish to cite from it. Please check the document version below.

Document Version
Publisher's PDF, also known as Version of record

Publication date:
2022

[Link to publication in University of Groningen/UMCG research database](#)

Citation for published version (APA):

Costanzo, A., Hildenbrandt, H., & Hemelrijk, C. K. (2022). Causes of variation of darkness in flocks of starlings, a computational model. *Swarm intelligence*, 16, 91-105. <https://doi.org/10.1007/s11721-021-00207-4>

Copyright

Other than for strictly personal use, it is not permitted to download or to forward/distribute the text or part of it without the consent of the author(s) and/or copyright holder(s), unless the work is under an open content license (like Creative Commons).

The publication may also be distributed here under the terms of Article 25fa of the Dutch Copyright Act, indicated by the "Taverne" license. More information can be found on the University of Groningen website: <https://www.rug.nl/library/open-access/self-archiving-pure/taverne-amendment>.

Take-down policy

If you believe that this document breaches copyright please contact us providing details, and we will remove access to the work immediately and investigate your claim.

Downloaded from the University of Groningen/UMCG research database (Pure): <http://www.rug.nl/research/portal>. For technical reasons the number of authors shown on this cover page is limited to 10 maximum.



Causes of variation of darkness in flocks of starlings, a computational model

A. Costanzo¹ · H. Hildenbrandt¹ · C. K. Hemelrijk¹

Received: 16 July 2020 / Accepted: 31 October 2021 / Published online: 25 November 2021
© The Author(s), under exclusive licence to Springer Science+Business Media, LLC, part of Springer Nature 2021

Abstract

The coordinated motion of large flocks of starlings is fascinating for both laymen and scientists. During their aerial displays, the darkness of flocks often changes, for instance dark bands propagate through the flock (so-called agitation waves) and small or large parts of the flock darken. The causes of dark bands in agitation waves have recently been shown to depend on changes in orientation of birds relative to the observer rather than changes in density of the flock, but what causes other changes in darkness need to be studied still and this is the aim of the present investigation. Because we cannot empirically relate changes in darkness in flocks to quantities, such as position and orientation of the flock and of its members relative to the observer, we study this in a computational model. We use StarDisplay, a model of collective motion of starlings, because its flocks resemble empirical data in many properties, such as their three-dimensional shape, their manner of turning, the correlation of heading of its group-members, and its internal structure regarding density and stability of neighbors. We show that the change in darkness in the flocks perceived by an observer on the ground mostly depends on the observer's distance to the flock and on the degree of exposure of the wing surface of flock members to the observer, and that darkness appears to decrease when birds roll during sharp turns. Remarkably, the darkness of the flock perceived by the observer was neither affected by the orientation of the flock relative to the observer nor by the density of the flock. Further studies are needed to investigate changes in darkness for flocks under predation.

Keywords Darkness in flocks · Flocking of birds · Collective motion · Video analysis · Computational modeling

✉ A. Costanzo
andreacostanzo881@gmail.com

H. Hildenbrandt
h.hildenbrandt@rug.nl

C. K. Hemelrijk
c.k.hemelrijk@rug.nl

¹ Faculty of Science and Engineering, Groningen Institute for Evolutionary Life Sciences (GELIFES), University of Groningen, Nijenborgh 7, 9747 AG Groningen, The Netherlands

1 Introduction

Collective motion (Vicsek et al. 2012, Couzin et al., 2002, Sumpter, 2010), and in particular the fascinating aerial displays of flocks of European starlings (*Sturnus vulgaris*), have attracted interdisciplinary scientific interest (Ballerini et al., 2008a, 2008b; Carere et al., 2009; Feare, 1984; Storms et al., 2019).

Contributing to this fascination are the fast changes in the darkness of a flock of starlings (Storms et al., 2019). They happen both in the absence of a predator and when the flock is under predator threat. Under such a threat, either a part of a flock turns dark momentarily or dark bands are propagating over the flock, the so-called agitation wave (Procaccini et al., 2011, Hemelrijk et al. 2015c). The question is how this affects the survival of the birds. Thus, we first need to know what the individual birds are doing. This has been investigated for the agitation wave. In starlings, an agitation wave starts as a reaction to an approach or attack by a predator, often a falcon (Storms et al., 2019). The wave moves away from it (Procaccini et al., 2011). Since these waves have been observed at large distance (of 1 km) of the observer, it was not clear whether they were ‘density’ waves (of individuals moving temporarily closer together as observed in herrings (Axelsen et al., 2001)) or waves of ‘orientation’ in which different surface-areas of the wing would be observed due to a skitter-like motion of the bird moving away from the predator. This would lead to a pattern resembling the waves due to rolling by dunlins in reaction to fright, but dunlins display different colors from belly and back (Potts, 1984). A computer simulation of flocks of starlings, StarDisplay, was used in order to understand what causes us to observe dark bands moving away from the predator. It revealed that we observe agitation waves due to a skitter-like escape motion where birds bank during their zig-like maneuver for escaping the predator (thus, an orientation wave) rather than a maneuver of fleeing forward into the flock away from the predator (a density wave). These bands resemble those in empirical data, qualitatively in their general appearance and quantitatively in their speed. Thus, agitation waves in starlings are waves of changes of orientation rather than of density (Hemelrijk et al. 2015c).

The causes of fluctuations in darkness in the absence of a predator have not been studied. We look at causes of such fluctuations when no predator is present. We investigate whether darkness fluctuations arise from temporal or spatial variation in density or the orientation of the members of a flock or the orientation of a flock as a whole, or a combination of these. For example, we hypothesize that a denser flock will appear darker. Another hypothesis is that observing an oblong flock along its longer axis should be perceived as darker than observing it along its shorter axis and a flock that turns should be darker than one that moves straight ahead, because when birds bank we observe a larger surface of the wing, like in agitation waves.

The aim of the present paper is to study what causes darkness to fluctuate (measured as average darkness of the entire flock) in the absence of a predator. This may help also understanding what happens during a predator attack when darkness changes differently from an agitation wave. Knowing what the birds are doing during darkness fluctuations will help to understand how and why darkness fluctuations affect the survival of the birds when attacked. Besides, a better understanding of the detailed motion of birds in large flocks has practical implications: it will help to develop techniques to drive a flock away (for example with robot falcons or drones) from a location where it is dangerous or causes damage, like airfields, airbases, and farming fields.

Several properties of the structure and dynamics of flocks of starlings have been investigated both experimentally (Major et al. 1978; Ballerini et al., 2008a, 2008b; Cavagna et al., 2010, 2013; Attanasi et al., 2015; Zoratto et al., 2010), e.g., by tracking positions of birds in flocks (Ballerini et al., 2008a), and theoretically (Bode et al. 2010; Bialek et al., 2012; Hildenbrandt et al., 2010; Hemelrijk et al. 2011; Hemelrijk et al. 2012; Pearce et al., 2014, Hemelrijk et al. 2015a, 2015b), e.g., by developing new models of collective motion that resemble real flocks (Hildenbrandt et al., 2010). To investigate causes of changes in darkness empirically requires tracking the positions and orientations of thousands of birds in flocks. Although there has been much progress on this recently (Cavagna et al., 2013; Nagy et al., 2010), for flocks of starlings it remains impossible if they comprise more than 5000 individuals. Therefore, we investigate darkness in a model of collective motion of starlings, StarDisplay (Hildenbrandt et al., 2010; Hemelrijk et al. 2015b). Using this particular model is justified, because its flocks resemble those of real birds in many traits, such as the distribution of angles and distances to the nearest neighbors (Hildenbrandt et al., 2010), the flat shape of flocks and their aspect ratio (Hildenbrandt et al., 2010), the way a flock turns (Hildenbrandt et al., 2010; Hemelrijk et al. 2012), the density distribution in the flock (Hildenbrandt et al., 2010), the scale-free correlation between correlation length of speed fluctuations and flock size (Hemelrijk et al. 2015b), and the instability of neighbors in a flock (Hemelrijk et al. 2015a).

We examine in the model how darkness of the flock, as measured by the signal received on a static camera, relates to the following quantities: The area of the flock (because it indicates group size and distance to the observer), aspect ratio of the flock (as an indication of asymmetry of its shape), the average nearest neighbor distance among flock members (as a measure of density), the distance of the center of the flock to the observer (as measure of distance to observer), the angle between the line of sight of the observer to the center of mass of the flock and the longest axis of the principal component analysis of the flock (representing the orientation of the flock) and the angle between the line of sight of the observer to the center of mass of the flock and the average orientation of birds (indicating the surface of the wings that is exposed to the observer).

In order to go beyond the range of densities and aspect ratios explored by our dynamical model, we also investigate a static model where birds are not moving and where they can be placed at any position such that the flock can have any desired density and aspect ratio.

2 Methods

2.1 Model

In our model of collective motion of starlings, StarDisplay (Hildenbrandt et al., 2010; Hemelrijk et al. 2015b), individuals are characterized by their position, heading, and orientation. The orientation is determined by the “up-vector,” which is a unit vector perpendicular to the surface of the wings (see Fig. 1a). The motion of birds is governed by two forces, a (social) steering force, similarly as in many models in the literature (Couzin et al., 2002, Strandburg-Peshkin et al. 2013, Pearce et al., 2014, Strombom 2011, Chate et al. 2008, Costanzo et al. 2018), and an aerodynamic force. The aerodynamic force is given by the sum of lift, drag, thrust, and gravity. Lift is perpendicular to the plane of the wings, while thrust and drag are, respectively, parallel and antiparallel to the direction of heading

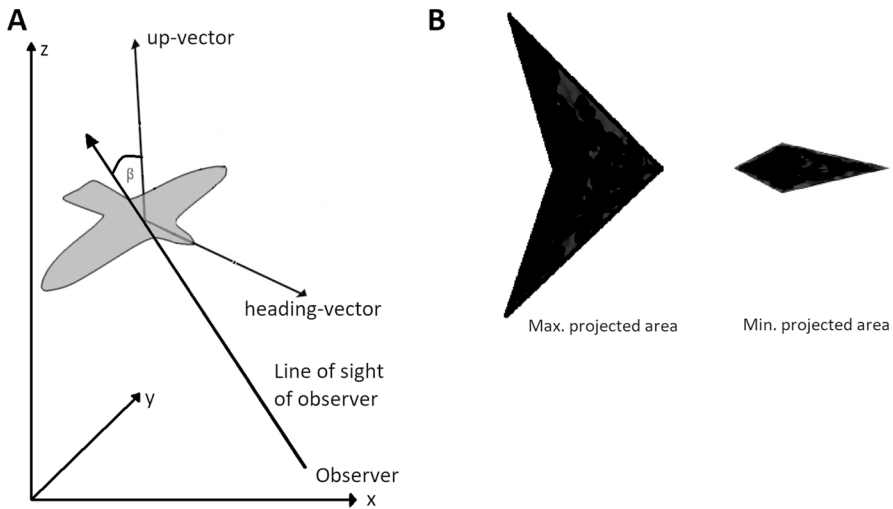


Fig. 1 **a** Sketch of one bird: Heading-vector and up-vector, which is orthogonal to the wing's surface. Angle β between the line of sight of the observer and the average up-vector of birds, $\beta \approx 0^\circ$ corresponds to a large exposed surface (e.g., bird with surface of wings parallel to the ground and flying above the observer), or bird with surface of wings orthogonal to the ground and flying in front of the observer), $\beta \approx 90^\circ$ corresponds to a low exposed surface. Figure modified with permission from (Hemelrijk et al. 2011). **b** Representation of the bird's projected area for two different views: maximum projected area to the observer (when the up-vector is parallel to the line of sight of the observer), and minimum projected area to the observer (when the up-vector is orthogonal to the line of sight of the observer), picture taken from (Hemelrijk et al. 2015c) and modified with permission

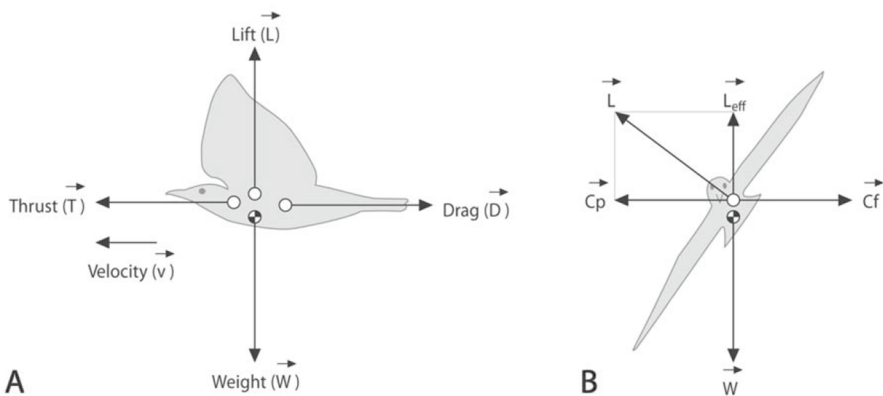


Fig. 2 Sketch of the forces acting on a bird flying straight (**a**) and banking (**b**). Birds bank in order to turn in a realistic way, taken from (Hemelrijk et al. 2011). C_p is the centripetal force, C_f is the centrifugal force, L is the lift (perpendicular to the plane of the wings), L_{eff} is the effective lift (antiparallel to the gravity)

(see Fig. 2). Wings are considered to be fixed without flapping. A lateral steering force in the model makes each bird roll into turns, followed by rolling back into position. Rolling in turns leads to a reduction in effective lift and thus, a loss in altitude, similar to what has been observed in empirical studies (Pomeroy et al. 1992; Gillies 2008).

Individuals interact with on average seven closest neighbors in their field of view (i.e., topological interaction). Individuals have a blind angle at the back (for parameter values see Table 1). The (social) steering force consists of avoidance of the closest neighbor in the field of view, attraction to the other interacting neighbors in the field of view, and alignment to their average heading. The steering force comprises also speed control, attraction to the roost and noise. The speed control causes birds to accelerate or decelerate toward the desired cruise speed. Attraction to the roost has a horizontal component toward the center of the roost, which is maximal when the bird is flying away from the roost and zero when it is flying toward it, and a vertical component attracting the birds to a specific altitude. It ensures that the flock does not fly far from the roost. The attraction to the roost has been modified compared to the original model (Hildenbrandt et al., 2010; Hemelrijk et al. 2015b) in order to get sharper turns more often. The direction of turns induced by the attraction to the roost is chosen randomly in order to avoid the almost circular motion around the roost observed in (Hildenbrandt et al.,

Table 1 Parameters used in the model StarDisplay

Parameter	Description	Value
<i>Generic</i>		
Δt	Integration time step	0.002 s
N	Number of birds	5000
<i>Of birds</i>		
Δu	Reaction time	0.019 s
v_0	Cruise speed	13.6 m/s
M	Mass	0.08 kg
C_L/C_D	Lift-drag coefficient	3.3
L_0	Default lift	0.78 N
D_0, T_0	Default drag, default thrust	0.24 N
$\omega\beta_{in}$	Banking control	2
$\omega\beta_{out}$	Banking control	0
T	Speed control	10 s
R_{max}	Maximum perception radius	200 m
n_c	Topological range	7.4
r_h	Radius of maximum separation (hard sphere)	0.4 m
r_{sep}	Separation radius	1.7 m
w_s	Weighting factor separation force	1 N
	Rear “blind angle” cohesion and alignment	36°
w_a	Weighting factor alignment force	1 N
w_c	Weighting factor cohesion force	1 N
w_ξ	Weighting factor random force	0.1 N
	Desired altitude	150 m
	Wing area	48 cm ²
	Wing aspect ratio	8.33
<i>Of roost</i>		
R_{roost}	Radius of roost	30 m
w_{RoostH}	Weighting factor horizontal attraction to the roost	0.00001 N
w_{RoostV}	Weighting factor vertical attraction to the roost	0.01 N/m

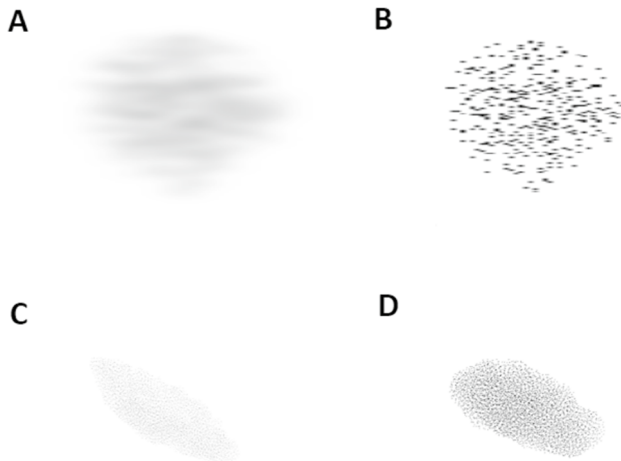


Fig. 3 Effect of applying a Gaussian filter on the image of a flock: **a** flock-image that is filtered and **(b)** the same image but not filtered. Snapshots of a **(c)** bright and a **(d)** dark flock. See Table 2 for corresponding measures

2010). We place the observer in the center of the roost so that the flock continues to be close. For a detailed description of the model, see (Hemelrijk et al. 2015b; Hildenbrandt et al., 2010); for parameter values, see Table 1.

2.2 Measurements and initial condition

To measure the global darkness of a moving flock, we generate a series of gray-scale images of it on a white background. We generate it from the perspective of an observer positioned on the ground either in the center of the roosting site (at position (0,0,0)) or at the side of it (at position (100,0,0), in order to keep the average distance of the flock from the observer constant at $d=215$ m in both cases of observer at the center and at the side) while looking at the center of the flock. In case a flock splits in multiple flocks, the observer orients itself toward the flock with the highest number of individuals. The field of view of the observer is 30° , representing a human observer using an optical zoom. We do this so that the flock occupies a sufficiently large proportion of the image. Individual birds are modeled as black delta-shaped objects with wing area of 48 cm^2 and wing aspect ratio of 8.33 (Fig. 1b).

We apply a Gaussian filter to the image (Fig. 3). Smoothing does not change the average luminance of the entire image (flock plus background). It causes white pixels that are between black ones to become gray. In this way, we can define the area A of the flock on the two-dimensional image as the number of non-white pixels divided by the total number of pixels of the image,

$$A = N_{\text{non-white}}/N$$

with $N=512^2$ being the total number of pixels of the image.

We measure darkness of the flock as

Table 2 Measures of the flocks shown in Fig. 3c and d

Measure	Of Fig. 3c	Of Fig. 3d
Darkness	0.04	0.11
Vertical component of the average orientation vector of birds up_z	0.92	1.00
Angle α between line of sight of the observer and longest axis of the flock	158°	147°
Area of the flock	0.005	0.009
Aspect ratio	3.03	1.75
Distance of the center of the flock from the observer d	319	259
Average nearest neighbor distance NND	1.30	1.25
Angle β between line of sight of the observer and average up-vector of birds	85°	58°

$$D_{flock} = 1 - \frac{\sum_{\text{non-white}} I_i}{N_{\text{non-white}} \cdot 255}$$

where I_i is the luminance of the i -th pixel, $\sum_{\text{non-white}} I_i$ is the sum of the luminance of the non-white pixels, and $N_{\text{non-white}}$ is the number of non-white pixels. A black pixel corresponds to a luminance of 0, and a white pixel corresponds to a luminance of 255. A darkness value close to 0 corresponds to a bright flock, and, respectively, a value close to 1 to a black flock.

Using the Gaussian filter, we introduce a decrease in darkness by increasing the distance to the flock (Figure Appendix 1). This is realistic, since an object that is further away can be seen with more difficulty, due to the fact that it will be less rich in contrast because of the larger volume of light-dispersing medium in between the onlooker and the object (Cronin et al., 2014.). Also, contrasts are stronger at the borders of the object, so larger objects (or objects closer to the observer) have more contrast and therefore, they are more visible.

This decrease in darkness with distance of the flock from the observer happens since the ratio between the perimeter of the flock and its area increases when the flock is further away from the observer. This reduces its darkness since the Gaussian filter acts on the perimeter of black areas, increasing the luminance of the black pixels.

The parameter sigma (i.e., the standard deviation of the Gaussian filter) affects the measure of darkness in the following way: A small value of σ ($\sigma = 0$) does not affect the luminance of the pixels and thus, is not appropriate to measure darkness, since without Gaussian filter the darkness would be always 1. A large value of σ ($\sigma = 100$) would make the contour of the flock-area too unprecise. The darkness decreases by increasing sigma (Figure Appendix 2). The value of sigma is chosen such that within the flock the white holes disappear. This happens at sigma = 3.

We initiate our simulations with 5000 birds with aligned headings and random positions in a spherical space. After a transition time of 10,000 steps (= 20 s), we begin our data collection. The transition time is used to let the flock develop from the spherical initial shape to an ellipsoidal shape. Every 100 steps, we record the darkness of the flock, along with its area (i.e., the share of non-white pixels in the image) and aspect ratio (i.e., the longest axis of the principal component analysis of the flock divided by the second longest axis of it). We also measure the average up-vector of birds (Fig. 1a) to quantify changes of orientation of birds, the average altitude of birds, and the average nearest neighbor distance (NND) among flock members as a measure of density.

Furthermore, we measure the distance d of the center of the flock to the observer, the angle α between the line of sight of the observer to the center of mass of the flock and the longest axis of the bounding box around it (computed with the principal component analysis of the positions of the birds) to study the effect on darkness of the orientation of the flock relative to the observer. The angle β between the line of sight of the observer to the center of mass of the flock and the average up-vector of birds (Fig. 1a) is used to study the effect on darkness of the orientation of individuals relative to the observer.

2.3 Static flocks

We also examine darkness in static flocks that do not move. In these, we set the position and orientation of individuals (in contrast to the model *StarDisplay*, where behavioral rules determine the locations of individuals). We vary the aspect ratio and density of flocks and give individual group-members the same heading- and up-vector while keeping the other parameters constant. When studying effects of the density, the perspective of the observer is from the ground (like for moving flocks) at distance from the flock $d=212$ m (similar to the average distance of moving flocks). When studying the aspect ratio, the observer is positioned on the ground and the longest axis of the bounding box around the flock is either parallel or orthogonal to the line of sight of the observer in order to maximize the difference in observed shape of the flock. While studying aspect ratio the distance of the flock from the observer is set to 350 m in order to study also large variations of the aspect ratio. For shorter distances and large aspect ratio (aspect ratio=9), the flock does not fit in the field of view of the observer.

2.4 Statistics

After excluding the first 10,000 steps (=20 s), for each of the 30 independent simulation runs of 200,000 steps (=400 s), we compute the Pearson product-moment correlation coefficient between darkness of the flock and the other measures. Subsequently, we compute the average and the variance of the correlation coefficients over the 30 runs (that have the same parameters and differ in their random starting positions).

3 Results

3.1 Flocks flying above the roosting site

The correlations that are strongest of all are the negative correlation between darkness and the angle β between the line of sight of the observer (positioned on the ground at the center of the roosting site), the positive correlation of darkness with the average up-vector of birds, and the negative correlation of darkness with the distance d of the flock from the observer (Fig. 4a red dots). This means that darkness mostly depends on the size of the wings' surface that is exposed to the observer and on distance to the observer rather than on density of the flock. Indeed darkness decreases when birds roll so that the flock turns sharply and increases when birds are flying straight without rolling (Fig. 5a). Darkness decreases during sharp turns since during a turn (either toward or away from the observer) there will be a point in time and space where the birds show minimal wings' surface to the observer. Darkness decreases with increasing distance d

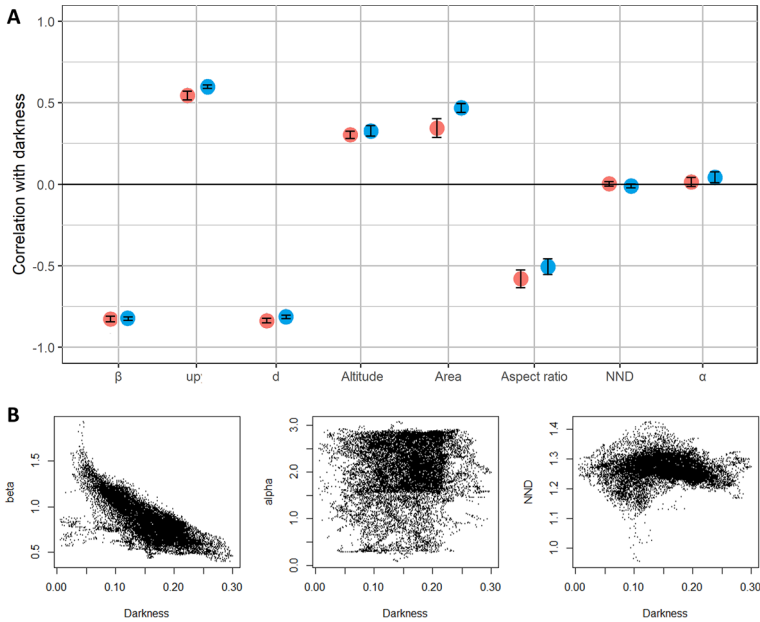


Fig. 4 **a** (top panel): Average value of the Pearson product-moment correlation between darkness and each of the following flock measures: angle β between observer’s line of sight and average up-vector of birds, the average vertical component of the up-vector of birds up_z , distance d of the flock center from the observer, altitude of the flock above ground, area of the flock, aspect ratio of the flock, average nearest neighbor distance NND, and angle α between line of sight of observer and longest axis of the principal component analysis of the flock. Red dots (with outer black circle): results when observer is located at the center, at position (0,0,0). Blue dots (without outer black circle): observer on the side, at position (100,0,0). **b** (bottom panels): Darkness as a function of the angle α between line of sight of observer and longest axis of the principal component analysis of the flock, angle β between observer’s line of sight and average up-vector of birds, the average vertical component of the up-vector of birds up_z , and the average nearest neighbor distance NND (complete dataset of the 10 runs) (Color figure online)

of the flock from the observer (Fig. 4a), as in empirical observations and measurements: the further away the flock, the more difficult it is to see it.

During turning, birds sink downwards somewhat because they lose lift while rolling. This causes observed darkness to decrease at lower altitude (Fig. 4a). When the area of the flock is smaller, the observed darkness decreases because this happens at larger distances d , and at larger distances the darkness decreases (Fig. 4a). The decrease in darkness with increasing aspect ratio of the flock (Fig. 4a) arises because flocks become brighter during sharp turns, and during sharp turns flocks become more elliptical (larger aspect ratio) (Fig. 5f). The larger aspect ratio during sharp turns is probably due to individuals sinking downwards because of the reduced lift when rolling.

In our model, darkness does not correlate with the density of the flock, measured by the average nearest neighbor distance among flock members, NND, nor with the orientation of the flock relative to the observer, as quantified by the angle α between the line of sight of the observer and the longest axis of the principal component analysis of the flock (Fig. 4a). Whether this may be due to the small range of values of the nearest neighbor distance and of the aspect ratio of the flock reached in our model of flying flocks, we investigate in section “Static flock.” Since a Pearson correlation coefficient

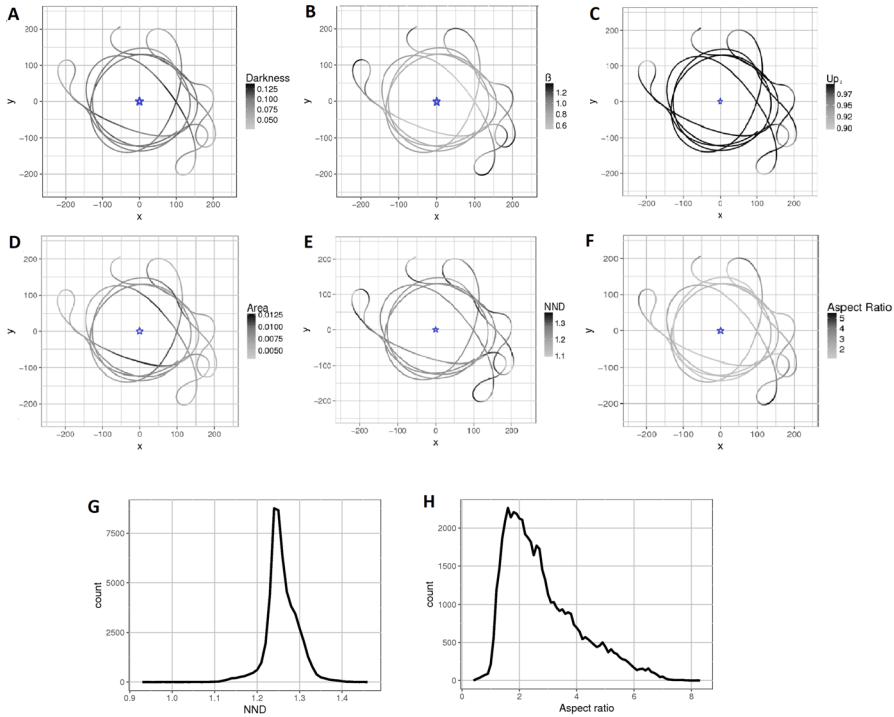


Fig. 5 Flock measures as a function of 2d-projection of the position of the center of mass of the moving flock. The observer is at the center of the roosting site, in position (0, 0, 0), indicated by a blue star. **a** Darkness. **b** Angle β between observer’s line of sight and average up-vector of birds. **c** Vertical component of the average orientation vector up_z . **d** Area of the flock. **e** Average nearest neighbor distance NND. **f** Aspect ratio of the flock. **g** Frequency distribution of the average nearest neighbor distance NND. **h** Frequency distribution of the aspect ratio of the flock

of zero does not suffice to conclude that two quantities are not correlated, we plot darkness as a function of the angle β , of the angle α , and of the average nearest neighbor distance among flock members NND, showing that NND and α do not correlate with darkness (Fig. 4b).

We get qualitatively similar results by observing the flock from the side at a distance of 100 m from the center of the roosting site (Fig. 4a blue dots), showing that the wing surface exposed to the observer influences the observed darkness independently from the location of the observer.

3.2 Static flocks

In order to study the effect of flock quantities (like density and aspect ratio) one by one, we use also static flocks, i.e., non-moving flocks where position and orientation of individuals is directly set by us, using a larger range of density and aspect ratio than the range we get for moving flocks. Here, we show that in contrast to our results on moving flocks, darkness increases with density and depends on the orientation of the flock relative to the observer. The observed darkness

decreases with average nearest neighbor distance (NND) (Fig. 6a). Besides, when the longest axis of the flock is oriented toward the observer (i.e., the angle α between observer's line of sight and longest axis of the flock is zero), the darkness is maximal, when the shortest axis of the flock is oriented toward the observer ($\alpha=90^\circ$) the darkness is minimal.

4 Discussion

Our results show that the distance of the flock from the observer and the orientation of birds relative to the observer are affecting darkness more than any of the other quantities. This is shown by the correlation between darkness and distance and the correlation between darkness and the angle β between the line of sight of the observer and the average up-vector of birds being the strongest correlations. The correlation between the orientation of birds and the observed darkness was expected, since the orientation of birds is also the cause of changes in darkness in case of the agitation waves. We also expected that for general changes in darkness (i.e., not specifically due to agitation waves) the density of the flock might have an important role, but we did not find correlations between the density of the flock and the observed darkness.

The effect of density and orientation of a flock relative to the observer on the observed darkness is much larger in our investigation of static flocks than moving flocks. This happens because the range of densities (NNDs) in moving flocks is much smaller than we use for static flocks and is too small to influence our observations of blackening (NND ranges from ca 0.9 to 1.5) (compare Figs. 5g and 6a). Similarly, the range in aspect ratio of moving flocks (see probability distribution function of the aspect ratio in Fig. 5h) is too small to affect the darkness. The values of densities and aspect ratios have been set by us in static flocks (with NND ranging from 0.5 to 2.0), but in the case of moving flocks we kept parameters of real flocks and these showed little variation in density and aspect ratio (see Table 1). Empirical measurements (covering a time interval of 7 s) on flocks flying in the absence of predators show a range of NND from 0.6 to 1.6 (Ballerini

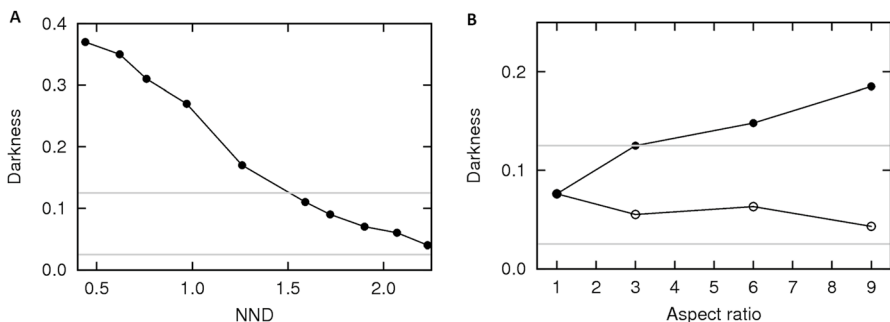


Fig. 6 Darkness of static flocks (a) Darkness as a function of average nearest neighbor distance NND in a spherical flock ($N=5000$, position of center of flock= $(150,0,150)$, position of observer= $(0,0,0)$, distance $d=212$ m) and (b) Darkness of an elongated flock ($N=5000$, $NND=1$, distance from the observer $d=350$ m, observer on the ground and flock at altitude 150 m) as a function of aspect ratio of the flock and orientation. Darkness is at its minimum when the flock orientation is orthogonal to the line of sight of the observer (empty symbols) and at its maximum when the flock orientation is parallel to the line of sight of the observer (filled symbols). Gray lines are the minimum and maximum values of darkness observed for moving flocks

et al., 2008a, 2008b), which we approximate by a range of NND from 0.9 to 1.5 (note that density is emergent in StarDisplay and cannot be set directly).

For static flocks, we chose ranges of values of NND and aspect ratio that are larger than in moving flocks, in order to show that these quantities do actually influence darkness. In moving flocks, these effects are negligible compared to the effect of other quantities, since the range of values that these quantities reach in moving flocks is not large enough. This could also be due to the fact that we consider global measures (i.e., average values on the entire flock), while sub-regions of the flock may reach local values that are beyond the observed range of the global variables.

The model StarDisplay that we used has 27 parameters (Table 1). The values of these parameters are chosen in a way that the flock resembles a real flock in many traits. We therefore consider our results to be robust and independent of simulation parameters as long as these are chosen in a way that the flock dynamic resembles real flocks of starlings. The number of individuals N might have an effect on the observed darkness, but it is beyond the scope of our study.

Despite that flocks of the model StarDisplay resemble real flocks in many traits, a limitation of the model is that it does not include flapping flight, but that it represents birds as rigid delta-shaped bodies. The effect of flapping of wings should be evaluated in future using a new model.

Limitations of our study are that it does not concern the adaptiveness of variation in darkness, and it does not concern the context of a flock being attacked by a predator. Blackening does not seem to be adaptive in the absence of a predator, it may be merely a side-effect of birds being asymmetrical. In the presence of a predator, blackening happens during wave events and otherwise (Carere et al., 2009; Procaccini et al., 2011; Storms et al., 2019; Zoratto et al., 2010). Wave events are reducing the catch success of the predator (Procaccini et al., 2011). Whether other blackening events in reaction to a predator, namely sudden changes in darkness of the flock, are adaptive and whether they also mainly depend on the surface of the wings exposed to the observer like when a predator is absent, needs further study.

In nature the dynamics of flocks are more rich than in our model because of the presence of multiple flocks, wind, birds of other species, and obstacles such as houses, and therefore, our model underestimates variation in darkness in reality. Our findings should be tested empirically by measuring darkness of real flocks and simultaneously tracking positions and orientations of single birds in flocks and of complete flocks.

We hope that our study, aimed at gaining understanding of the internal dynamics of flocks of starlings, specifically the processes underlying temporal and spatial changes in darkness, contributes to the interest in aerial displays of huge flocks of starlings known to so many of us, laymen and scientists alike.

Appendix

In the appendix we show additional graphs reporting the darkness as a function of the distance d from a static flock of 10.000 individuals (Fig. 7) and the darkness as a function of the parameter σ of the Gaussian filter (Fig. 8).

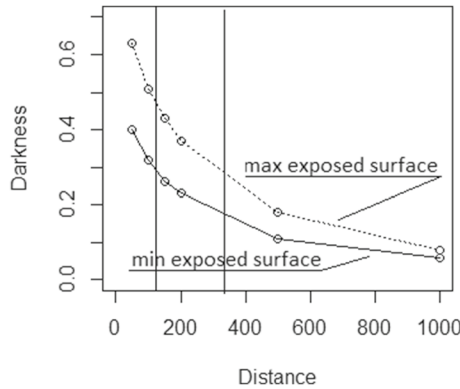


Fig. 7 Darkness as a function of distance d from the static flock of 10,000 individuals. Dashed line: flock showing maximal wing surface: center of mass of the flock at $(0,0,d)$, average heading vector $(1,0,0)$, average up vector $(0,0,1)$, and camera at $(0,0,0)$. Solid line: flock showing minimal wing surface center of mass of the flock at $(d,0,150)$, average heading vector $(1,0,0)$, average up vector $(0,0,1)$, and camera at $(0,0,150)$. Solid vertical lines are guides to the eye that indicate the range of distances reached in the simulations of moving flocks

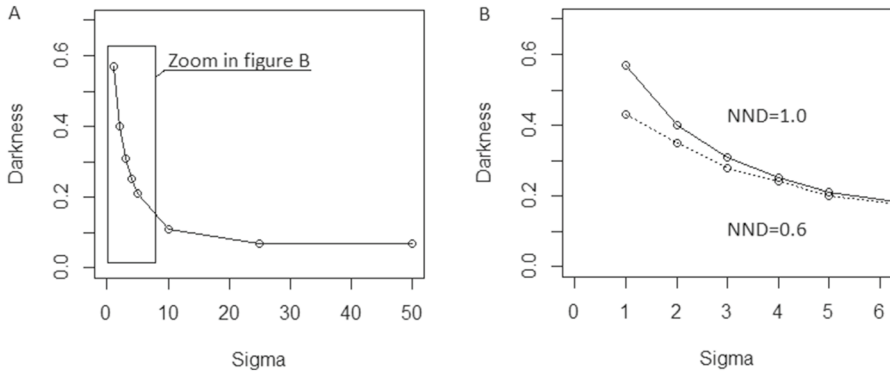


Fig. 8 Darkness as a function of the parameter sigma of the Gaussian filter. Flock of 10,000 individuals with center of mass at $(0,0,250)$, mean heading vector $(1,0,0)$, and mean up vector $(0,0,1)$, $NND=0.6$ (dashed lines) and $NND=1.0$ (solid lines). Right panel is a zoom on same data. The value of $\sigma=3$ chosen for our simulations is a value small enough to get a difference in darkness for different nearest neighbor distances, which confirms that the value of $\sigma=3$, that was chosen so that the flock was considered as a whole, because white pixels between birds become non-white, is a good choice for our simulations. A smaller value of sigma would produce white pixels between birds such that we could not identify and measure the area of the flock. A larger value of sigma would have the negative effect of flocks with unprecise contours and flocks with different nearest neighbor distances producing the same darkness

Supplementary Information The online version contains supplementary material available at <https://doi.org/10.1007/s11721-021-00207-4>.

Funding This study was funded by NWO-TTW (Netherlands Organization for Scientific Research), Project nr 14723.

Declarations

Conflict of interest The authors declare that they have no conflict of interest.

Ethical approval This article does not contain any studies with human participants or animals performed by any of the authors.

Consent for publication All author gave their consent.

Data availability <https://doi.org/10.6084/m9.figshare.8273549>

Code availability Available upon request.

References

- Attanasi, A., Cavagna, A., Del Castello, L., Giardina, I., Jelic, A., Melillo, S., Parisi, L., Pohl, O., Shen, E., & Viale, M. (2015). Emergence of collective changes in travel direction of starling flocks from individual birds' fluctuations. *Journal of the Royal Society Interface*, *12*(108), 20150319.
- Axelsen, B. E., Anker-Nilssen, T., Fossum, P., Kvamme, C., & Nøttestad, L. (2001). Pretty patterns but a simple strategy: Predator-prey interactions between juvenile herring and Atlantic puffins observed with multibeam sonar. *Canadian Journal of Zoology*, *79*(9), 1586–1596.
- Ballerini, M., Cabibbo, N., Candelier, R., Cavagna, A., Cisbani, E., Giardina, I., Orlandi, A., Parisi, G., Procaccini, A., Viale, M., & Zdravkovic, V. (2008a). Empirical investigation of starling flocks: A benchmark study in collective animal behaviour. *Animal Behaviour*, *76*(1), 201–215.
- Ballerini, M., Cabibbo, N., Candelier, R., Cavagna, A., Cisbani, E., Giardina, I., Lecomte, V., Orlandi, A., Parisi, G., Procaccini, A., Viale, M., & Zdravkovic, V. (2008b). Interaction ruling animal collective behavior depends on topological rather than metric distance: Evidence from a field study. *Proceedings of the National Academy of Sciences*, *105*(4), 1232–1237.
- Bialek, W., Cavagna, A., Giardina, I., Mora, T., Silvestri, E., Viale, M., & Walczak, A. M. (2012). Statistical mechanics for natural flocks of birds. *Proceedings of the National Academy of Sciences*, *109*(13), 4786–4791.
- Bode, N. W., Franks, D. W., & Wood, A. J. (2011). Limited interactions in flocks: Relating model simulations to empirical data. *Journal of the Royal Society Interface*, *8*(55), 301–304.
- Carere, C., Montanino, S., Moreschini, F., Zoratto, F., Chiarotti, F., Santucci, D., & Alleva, E. (2009). Aerial flocking patterns of wintering starlings, *Sturnus vulgaris*, under different predation risk. *Animal Behaviour*, *77*(1), 101–107.
- Cavagna, A., Cimarelli, A., Giardina, I., Parisi, G., Santagati, R., Stefanini, F., & Viale, M. (2010). Scale-free correlations in starling flocks. *Proceedings of the National Academy of Sciences*, *107*(26), 11865–11870.
- Cavagna, A., Queirós, S. D., Giardina, I., Stefanini, F., & Viale, M. (2013). Diffusion of individual birds in starling flocks. *Proceedings of the Royal Society B: Biological Sciences*, *280*(1756), 20122484.
- Chaté, H., Ginelli, F., Grégoire, G., Peruani, F., & Raynaud, F. (2008). Modeling collective motion: Variations on the Vicsek model. *The European Physical Journal B*, *64*(3–4), 451–456.
- Cleveland Bent, A. (1927). *Life histories of North American shore birds (No. 598.3397 C5)*. Dover Publications.
- Cronin, T. W., Johnsen, S., Marshall, N. J., & Warrant, E. J. (2014). *Visual ecology*. Princeton University Press.
- Davis, J. M. (1980). The coordinated aerobatics of dunlin flocks. *Animal Behaviour*, *28*(3), 668–673.
- Costanzo, A., & Hemelrijk, C. K. (2018). Spontaneous emergence of milling (vortex state) in a Vicsek-like model. *Journal of Physics D: Applied Physics*, *51*(13), 134004.

- Couzin, I. D., Krause, J., James, R., Ruxton, G. D., & Franks, N. R. (2002). Collective memory and spatial sorting in animal groups. *Journal of Theoretical Biology*, 218(1), 1–11.
- Feare, C. J. (1984). *The starling*. Oxford University Press.
- Gillies, J., Bacic, M., Thomas, A., Taylor, G., & Yuan, F. (2008). Modeling and identification of steppe eagle (*Aquila nipalensis*) dynamics. In: AIAA Modeling and Simulation Technologies Conference and Exhibit (p. 7096).
- Hemelrijk, C. K., & Hildenbrandt, H. (2011). Some causes of the variable shape of flocks of birds. *PLoS one*, 6(8), e22479.
- Hemelrijk, C. K., & Hildenbrandt, H. (2012). Schools of fish and flocks of birds: Their shape and internal structure by self-organization. *Interface Focus*, 2(6), 726–737.
- Hemelrijk, C. K., & Hildenbrandt, H. (2015). Diffusion and topological neighbours in flocks of starlings: Relating a model to empirical data. *PLoS One*, 10(5), e0126913.
- Hemelrijk, C. K., & Hildenbrandt, H. (2015b). Scale-free correlations, influential neighbours and speed control in flocks of birds. *Journal of Statistical Physics*, 158(3), 563–578.
- Hemelrijk, C. K., van Zuidam, L., & Hildenbrandt, H. (2015). What underlies waves of agitation in starling flocks. *Behavioral Ecology and Sociobiology*, 69(5), 755–764.
- Hildenbrandt, H., Carere, C., & Hemelrijk, C. K. (2010). Self-organized aerial displays of thousands of starlings: A model. *Behavioral Ecology*, 21(6), 1349–1359.
- Krause, J., Ruxton, G. D., Ruxton, G., & Ruxton, I. G. (2002). *Living in groups*. Oxford University Press.
- Kunz, H., Züblin, T., & Hemelrijk, C. K. (2006). On prey grouping and predator confusion in artificial fish schools. In: Proceedings of the Tenth International Conference of Artificial Life. MIT Press, Cambridge, Massachusetts.
- Nagy, M., Ákos, Z., Biro, D., & Vicsek, T. (2010). Hierarchical group dynamics in pigeon flocks. *Nature*, 464(7290), 890–893.
- Pearce, D. J., Miller, A. M., Rowlands, G., & Turner, M. S. (2014). Role of projection in the control of bird flocks. *Proceedings of the National Academy of Sciences*, 111(29), 10422–10426.
- Major, P. F., & Dill, L. M. (1978). The three-dimensional structure of airborne bird flocks. *Behavioral Ecology and Sociobiology*, 4(2), 111–122.
- Procaccini, A., Orlandi, A., Cavagna, A., Giardina, I., Zoratto, F., Santucci, D., Chiarotti, F., Hemelrijk, C. K., Alleva, E., Parisi, G., & Carere, C. (2011). Propagating waves in starling, *Sturnus vulgaris*, flocks under predation. *Animal Behaviour*, 82(4), 759–765.
- Pomeroy, H., & Heppner, F. (1992). Structure of turning in airborne rock dove (*Columba livia*) flocks. *The Auk*, 109(2), 256–267.
- Potts, W. K. (1984). The chorus-line hypothesis of manoeuvre coordination in avian flocks. *Nature*, 309(5966), 344–345.
- Storms, R. F., Carere, C., Zoratto, F., & Hemelrijk, C. K. (2019). Complex patterns of collective escape in starling flocks under predation. *Behavioral Ecology and Sociobiology*, 73(1), 10.
- Strandburg-Peshkin, A., Twomey, C. R., Bode, N. W., Kao, A. B., Katz, Y., Ioannou, C. C., & Couzin, I. D. (2013). Visual sensory networks and effective information transfer in animal groups. *Current Biology*, 23(17), R709–R711.
- Sumpter, D. J. (2010). *Collective animal behavior*. Princeton University Press.
- Vicsek, T., & Zafeiris, A. (2012). Collective motion. *Physics Reports*, 517(3–4), 71–140.
- Zoratto, F., Carere, C., Chiarotti, F., Santucci, D., & Alleva, E. (2010). Aerial hunting behaviour and predation success by peregrine falcons *Falco peregrinus* on starling flocks *Sturnus vulgaris*. *Journal of Avian Biology*, 41(4), 427–433.